

## Excited states and energy relaxation in stacked InAs/GaAs quantum dots

R. Heitz

*Photonic Materials and Devices Laboratory, University of Southern California, Los Angeles, California 90089-0241  
and Institut für Festkörperphysik, Technische Universität Berlin, Hardenbergstrasse 36, D-10623 Berlin, Germany*

A. Kalburge and Q. Xie

*Photonic Materials and Devices Laboratory, University of Southern California, Los Angeles, California 90089-0241*

M. Grundmann

*Institut für Festkörperphysik, Technische Universität Berlin, Hardenbergstrasse 36, D-10623 Berlin, Germany*

P. Chen

*Photonic Materials and Devices Laboratory, University of Southern California, Los Angeles, California 90089-0241*

A. Hoffmann

*Institut für Festkörperphysik, Technische Universität Berlin, Hardenbergstrasse 36, D-10623 Berlin, Germany*

A. Madhukar

*Photonic Materials and Devices Laboratory, University of Southern California, Los Angeles, California 90089-0241*

D. Bimberg

*Institut für Festkörperphysik, Technische Universität Berlin, Hardenbergstrasse 36, D-10623 Berlin, Germany*

(Received 18 August 1997)

Excited states and energy relaxation processes are studied for stacked InAs/GaAs QD's with GaAs cap layers grown by migration enhanced epitaxy. Photoluminescence excitation (PLE) spectra reveal the excited state spectrum as a function of size for self-assembled InAs QD's in multilayered samples with 36-ML spacers. The observed energy shifts and splittings are consistent with those of hole states numerically calculated for pyramidal QD's supporting assignment to the transition between the electron ground  $|000\rangle$  and the  $|001\rangle$  excited hole state. The optical results suggest the island shape uniformity to improve in multilayered samples, which is attributed to the contribution of the buried islands to the surface strain altering the island formation kinetics and energetics that also underlie vertical self-organization. Time-resolved photoluminescence (TRPL) results yield a lifetime of 40 ps for the first excited  $|001\rangle$  hole state, attributed to multiphonon relaxation processes bridging the approximately 100 meV level separation, and ground-state lifetimes around 700 ps independent of the detection energy. At high excitation densities saturation of QD states leads to long-living excited-state PL and up to 1 ns delay in the ground-state PL decay, showing radiative decay to be the dominant recombination process in the QD's. The results presented contribute to the understanding of PLE spectra of an inhomogeneous QD ensemble, which is argued to be sensitive to the shape uniformity, the excited-state spectrum, and competing recombination processes. [S0163-1829(98)03115-4]

### I. INTRODUCTION

The spontaneous formation of *coherent* three-dimensional (3D) islands in highly strained semiconductor epitaxy such as  $\text{In}_x\text{Ga}_{1-x}\text{As}$  on GaAs (Ref. 1) and SiGe on Si (Ref. 2) has attracted interest as nature's way to generate nm-scale quantum dots (QD's). Above a critical deposition thickness, coherent  $\text{In}_x\text{Ga}_{1-x}\text{As}$  islands with lateral extensions of 10–20 nm and heights of 5–10 nm are spontaneously formed on top of a 2D layer, called the wetting layer (WL).<sup>3–7</sup> Although the formation of 3D islands following a WL, referred to as the Stranski-Krastanow growth mode, is long known in strained epitaxy,<sup>8</sup> only the discovery of the defect-free coherent nature of the islands<sup>1,2</sup> revealed the potential of the small QD's formed after GaAs overgrowth for optoelectronic applications. The demonstration of QD-based injection lasers,<sup>9–11</sup>

with threshold current densities down to some  $10 \text{ A cm}^{-2}$  and the predicted<sup>12</sup> high-temperature stability, shows the high optical quality of the QD structures. However, self-assembled QD's suffer  $\sim 10\%$  size fluctuation<sup>3–7</sup> as well as shape nonuniformity<sup>13</sup> smearing out the otherwise discrete density of states. The nonuniformity of self-assembled QDs makes a detailed investigation of the excited state spectrum and of energy relaxation (and recombination) processes difficult, which are both of basic physical interest and critical for design and performance of devices.

The excited-state spectrum of self-assembled QD's as well as the corresponding optical transitions are still controversial. Depending on the assumed QD shape and size, calculations predict the observation of "allowed" transitions between electron and hole states of the same quantum number<sup>14–16</sup> or recombination of holes in various excited

states with electrons in the ground state.<sup>17–19</sup> In the latter case, the low QD symmetry accounts for the oscillator strength of the otherwise “forbidden” transitions. Experimental information on excited states of self-assembled QD’s is based on photoluminescence (PL) spectra at excitation densities sufficient to saturate QD states<sup>19–22</sup> and on capacitance measurements.<sup>14,23</sup> These experiments probe QD’s charged with multiple electron-hole pairs or carriers, respectively, and thus the single-particle states are altered by Coulomb interaction.<sup>24,25</sup> Highly sensitive absorption techniques, like calorimetric absorption spectroscopy, are able to resolve ground- and excited-state transitions of unpopulated QD’s,<sup>26</sup> but are limited by the inhomogeneous broadening. Optical techniques such as selectively excited PL (Refs. 14,20) or PL excitation (PLE) (Refs. 6,13) spectroscopy are expected to reveal excited-state transitions and the size dependence of the excited-state splitting. However, nonradiative recombination in competing QD samples has been demonstrated to result in the observation of multiphonon resonances.<sup>13,27</sup>

The discrete atomlike energy spectrum of QD’s imposes constraints for inelastic phonon scattering that have been proposed to slow down carrier relaxation.<sup>28,29</sup> Indeed, interlevel scattering times of the order of some 10 ps have been observed in time-resolved PL (TRPL) excitation measurements.<sup>27,30</sup> The correspondingly long relaxation-limited lifetime of the excited states makes PLE sensitive to competing radiative and nonradiative recombination processes, which ultimately might suppress ground state PL, the so-called phonon bottleneck effect.<sup>28</sup> In an inhomogeneous QD sample the phonon bottleneck effect leads to multiphonon resonances in the PLE spectra, allowing only QD’s with fast intradot relaxation to contribute to the PLE signal.<sup>27</sup> It is not clear yet if the competing relaxation process is intrinsic to small QD’s presenting a principal limit to the achievable quantum yield.

The growth of multilayered QD structures has increasingly attracted interest. Depending on the spacer thickness between subsequent QD layers vertical self-organization of islands in stacks has been observed.<sup>31</sup> The contribution of the buried islands, acting as stressors, to the surface strain field leads to strain-driven In migration favoring formation of new islands on top of the buried ones.<sup>31,32</sup> Although vertical ordering of  $\text{In}_x\text{Ga}_{1-x}\text{As}$  3D islands in  $\text{In}_x\text{Ga}_{1-x}\text{As}/\text{GaAs}$  multilayered structures was noted early on,<sup>33</sup> the highly defected nature of the material did not draw attention to the potential of vertical self-organization. The high volume density of islands in multilayered structures has been exploited in QD injection lasers.<sup>9,10,11</sup> The formation of vertically ordered island stacks allows to exploit electronic coupling of the islands by controlling the inter-island separation in the nm region.<sup>11,34</sup> Recent results for the  $\text{SiGe}/\text{Si}$  system suggest that vertical self-organization might improve the uniformity of self-assembled islands in the upper layers,<sup>35,36</sup> making stacking a promising means to improve the island uniformity.

In this paper we report on PLE and TRPL investigations of stacked  $\text{InAs}/\text{GaAs}$  QD’s in multilayered samples with  $\text{GaAs}$  spacers grown by migration enhanced epitaxy (MEE). The optical results suggest vertical self-organization improves, in addition to the size, also the shape uniformity of

the islands found. Additionally, nonradiative recombination for samples with MBE grown caps is negligible for these samples.<sup>27</sup> The higher uniformity of the QD’s in the multilayered samples, together with the lack of nonradiative recombination, allows the observation of the QD size-dependent excited-state splitting and the study of the intrinsic carrier relaxation and recombination dynamics of the self-assembled  $\text{InAs}/\text{GaAs}$  QD’s.

## II. SAMPLES AND EXPERIMENTAL SETUP

The samples were grown in a solid source RIBER molecular-beam epitaxy (MBE) system on semi-insulating  $\text{GaAs}(001) \pm 0.1^\circ$  substrates covered with a high-quality undoped  $\text{GaAs}$  buffer layer as described in Refs. 31 and 37.  $\text{InAs}$  was deposited at  $500^\circ\text{C}$ , a growth rate of  $0.22 \text{ ML}\cdot\text{s}^{-1}$ , and an As partial pressure of  $6 \times 10^{-6}$  Torr on a starting surface showing clear  $c(4 \times 4)$  reconstruction. The reflection high-energy electron diffraction pattern became spotty after  $\sim 1.57 \text{ ML}$   $\text{InAs}$  deposition indicating the 2D to 3D morphology transition. The total deposition per  $\text{InAs}$  layer was  $1.74 \text{ ML}$ , resulting in a lateral QD density of  $\sim 300 \mu\text{m}^{-2}$ . For multilayered samples, 20- and 36-ML-thick  $\text{GaAs}$  spacers were grown at  $400^\circ\text{C}$  by MEE after each  $\text{InAs}$  deposition. Finally, the samples were capped with 170-ML MEE-grown  $\text{GaAs}$ . The use of MEE for the growth of the  $\text{GaAs}$  spacer and cap layers improves the PL yield of the QD’s.<sup>6</sup> The 20- and 36-ML  $\text{GaAs}$  spacers reestablish a planar growth surface completely burying the  $\text{InAs}$  islands<sup>6</sup> and result in vertical ordering ( $>95\%$ ) of the  $\text{InAs}$  islands in stacks.<sup>31</sup>

For the PL and PLE experiments the samples were mounted in a continuous-flow He cryostat. PL was excited by an  $\text{Ar}^+$  laser or a tungsten lamp dispersed by a  $0.27\text{-m}$  double-grating monochromator as tunable, low excitation density ( $<0.02 \text{ W cm}^{-2}$ ) light source and detected through a  $0.5\text{-m}$  single-grating monochromator using a cooled Ge diode. The TRPL measurements were performed in superfluid He with a Ti-sapphire laser providing 150 fs pulses at a repetition rate of 76 MHz for excitation and a  $0.35\text{-m}$  subtractive double-grating monochromator in combination with an infrared-enhanced streak camera for detection. The full width at half the maximum (FWHM) of the system response to the excitation pulses was between 25 and 60 ps depending on the time-range setting. Time constants down to 5 ps could be resolved taking into account the system response to the excitation pulses.

## III. EXCITED STATES OF STACKED $\text{InAs}$ QUANTUM DOTS

Low excitation density PL spectra of the multilayered samples (Fig. 1) show a systematic effect of the arrangement of QD’s in stacks. The QD PL centered at  $1.186 \text{ eV}$  with a FWHM of  $70 \text{ meV}$  for the single-layer sample exhibits a redshift and becomes narrower with increasing number of layers. The QD PL peak in the five-layer, 36-ML spacer, sample is  $87\text{-meV}$  redshifted and nonsymmetric. PL spectra at moderate excitation densities of  $1\text{--}10 \text{ W cm}^{-2}$ , Fig. 2(a), reveal a doublet structure with peaks at  $1.099$  and  $1.138 \text{ eV}$ . At high excitation densities the  $1.138\text{-eV}$  peak domi-

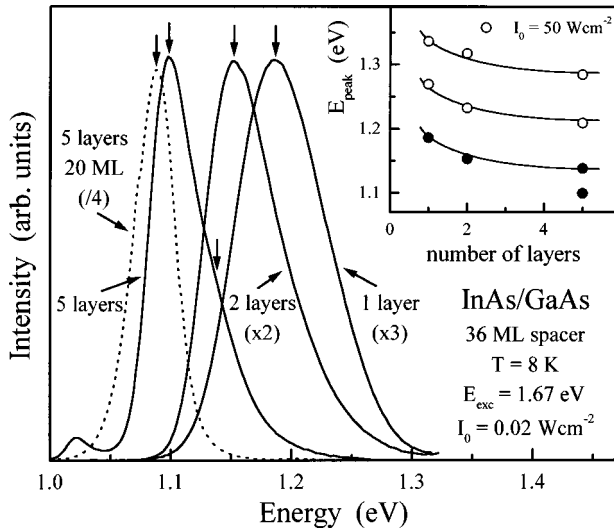


FIG. 1. PL spectra for multilayered InAs/GaAs samples with 36-ML spacers (full lines) excited nonresonantly in the GaAs barrier. The PL spectrum of the five-layer sample with 20-ML spacers (dashed line) is given for comparison and the vertical arrows mark the detection positions for the PLE spectra shown in Fig. 3. The inset gives the PL peak positions observed for low (solid circles) and high (open circles) excitation densities. The lines are for optical guidance only.

nates and excited state transitions are observed. As will be shown below, these peaks are distinguished by a different excitation behavior and decay dynamics, suggesting the presence of two different types of QD's in the five-layer sample with 36-ML spacers. As discussed in more detail below, we propose a systematic variation of the island shape along the stacks to result in a transition from uncoupled to coupled QD's with different electronic properties leading to the ob-

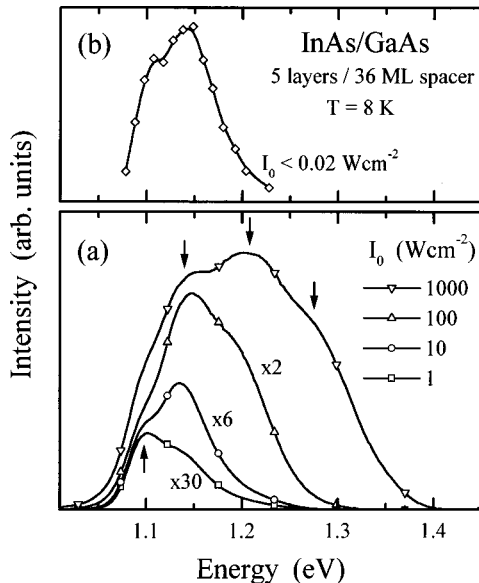


FIG. 2. Panel (a) shows the PL of the five-layer sample with 36-ML spacers for different excitation densities excited with a cw  $\text{Ar}^+$  laser. Panel (b) shows the PL intensity for low-density excitation in the 100 meV excited state resonance showing that the peak centered at 1.138 eV, which dominates the PL at  $10 \text{ W cm}^{-2}$ , results from the ground-state transition of uncoupled QD's in the stacks.

served PL doublet structure. Energy transfer within the stack quenches the PL of the higher-energy uncoupled QD's at low excitation densities. Reducing the spacer thickness to 20 ML (dashed spectrum in Fig. 1), only the low-energy peak at 1.088 eV remains with an almost Gaussian line shape and a FWHM of 36 meV. The inset in Fig. 1 summarizes for samples with 36-ML spacers the ground-state transition energies (solid circles) and the excited-state transition energies (open circles) observed in high excitation density PL experiments (Fig. 2; not shown for the one- and two-layer samples).

The formation of a QD superlattice due to electronic coupling within the QD stacks has been invoked to explain comparable low energy shifts observed for multilayered samples with GaAs spacers of thickness 18 ML or less.<sup>11,34</sup> The coupling strength depends on the wave-function overlap and thus decreases exponentially with increasing thickness of the GaAs barrier between the vertically aligned InAs QD's. In that respect, the only 11-meV energy difference between the QD PL transitions at 1.088 and 1.099 eV for five-layer samples with 20- and 36-ML spacers, respectively, seems rather small, particularly since the 20-ML spacers are only slightly thicker than the average island height of 5.5 nm observed in AFM studies for single layer samples,<sup>7</sup> whereas the 36-ML spacers are expected to result in about 5-nm GaAs barriers from the QD tip. Obviously, the barrier thickness is a function of the QD shape (for a given volume) and, as argued below, the islands tend to become steeper with increasing layer number leading to a decreasing barrier thickness in the upper layers of the stacks. We propose the coexistence of coupled and uncoupled QD's in the five-layer sample with 36-ML spacers as giving rise to the PL peaks centered at 1.099 and 1.138 eV, respectively. The energy shifts with respect to the single layer sample indicate that electronic coupling accounts only for part of the stacking-induced low-energy shift of the QD ground state transition energy.

Ledentsov *et al.*<sup>11</sup> proposed vertical In transfer between stacked InAs layers for their samples having thin GaAs spacer layers ( $\leq 4.5 \text{ nm}$ ) insufficient to completely cover the QD's. The transfer was attributed to the tendency of InAs to wet the exposed GaAs surface. The increase in InAs coverage in the higher layers increases the average island size. However, in the present samples the GaAs spacer layers completely bury the InAs islands and reestablish a flat growth front<sup>6</sup> making vertical mass transfer unlikely. The strain-induced surface migration leading to vertical self-organization could increase the island volume at the expense of the WL. Indeed, the 2D to 3D morphology transition involves the transfer of InAs already incorporated in the 2D layer to the growing islands<sup>38</sup> and at 1.74-ML deposition the 3D islands reside on a high-quality 1-ML InAs WL,<sup>39</sup> much thinner than the critical coverage of 1.57 ML for InAs island formation. Figure 3 shows PLE spectra for the multilayered samples with 36-ML spacers (full lines). The respective detection energies are indicated by vertical arrows in Fig. 1. The PLE spectra show two excitation resonances at 1.45 and 1.49 eV, which we attribute to the heavy (hh) and light (lh) hole transitions of the InAs quantum well formed by the WL. The transition energies indicate a WL thickness of about 1 ML.<sup>40,41</sup> The energy of the WL does not shift with the de-

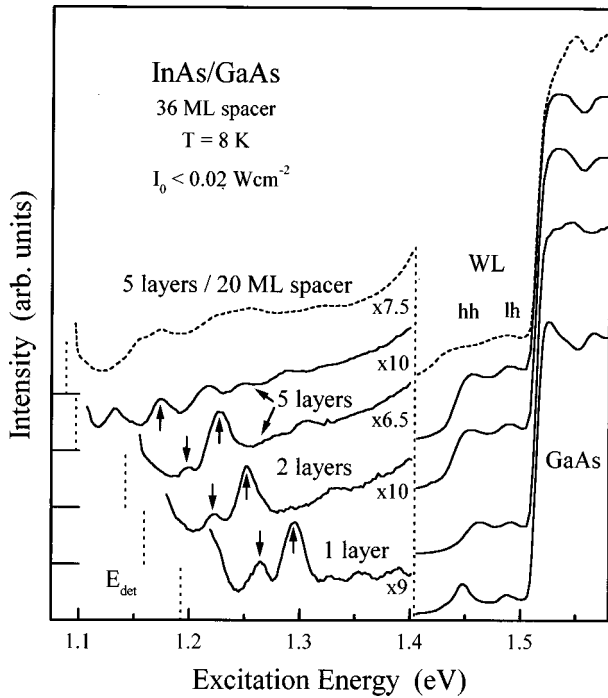


FIG. 3. PLE spectra for multilayered InAs/GaAs samples with 36-ML spacers (full lines). The PLE spectrum of the five-layer sample with 20-ML spacers (dashed line) is given for comparison. The detection energies are marked by arrows in Fig. 1. The PLE spectra are normalized for nonresonant excitation at 1.67 eV and shifted in the  $y$  direction for clarity. The combined experimental resolution for detection and excitation was better than 5 meV.

tection energy (compare, e.g., the two spectra for the five-layer sample with 36-ML spacers shown in Fig. 3) indicating that the effective WL thickness is the same for all layers. Together with the almost perfect vertical correlation of the islands,<sup>31</sup> i.e., a constant island density in the various layers, the results suggest that the *average* island volume does not change significantly in the stacking process.

The arrangement of InAs islands in stacks, however, allows the InAs QD's to relieve more strain than in the case of isolated QD's in single layer samples.<sup>11,42</sup> As a result the InAs band gap energy will decrease leading to a low-energy shift of the QD transition energies. This is supported by the PL spectra (Fig. 1) showing that even QD's in the first InAs layer experience a redshift in the stacks, which is expected only in case of electronic coupling or an altered strain situation. The analysis of the electronic coupling in QD stacks needs to take into account the altered strain relaxation as proposed in Refs. 11 and 42.

Returning to the three lowest PLE spectra depicted in Fig. 3 for samples with one, two, and five InAs layers with 36-ML spacers, the general shapes are remarkably similar, supporting the notion of uncoupled QD's in the stacks. The PLE spectra are normalized at 1.67 eV and shifted in the  $y$  direction for clarity. The high excitation efficiency for excitation above the GaAs band gap shows the high carrier capture efficiency of the InAs/GaAs QD's.<sup>13</sup> The PLE efficiency drops about one decade for excitation below the GaAs band gap, reflecting the lower optical thickness of the WL. The integrated intensity of the WL excitation increases in comparison to the GaAs excitation efficiency with increasing

number of stacks due to the contributions of the various InAs layers. Exciting below the hh-WL resonance at 1.45 eV the PLE efficiency decreases again by approximately one decade. To the excitation in this energy region contribute only excitation processes localized at the QD's: either excited state transitions or charge transfer transitions leaving one carrier localized in the QD and the other in the WL followed by the immediate recapture of the photoexcited carrier by the now charged QD. The two characteristic PLE resonances (indicated by vertical arrows in Fig. 3) located about 60 and 100 meV above the detection energy with FWHM's of about 25 meV are attributed to excited-state absorption of the QD's.<sup>6,13,27,43</sup> Near the detection energy stray light in the PLE system leads to the rising signal hampering the detection of resonant excitation of the QD ground state or of excitation resonances close to the detection energy. However, PLE spectra for the one- and two-layer samples excited with a tunable Ti-sapphire laser reveal only Raman scattering of GaAs TO and LO phonons within 40 meV of the detection energy.

Figure 4 compares contour plots of the PL intensity as function of the detection energy and the excess excitation energy  $\Delta E = E_{\text{exc}} - E_{\text{det}}$  for the one-, two-, and five-layer samples with 36-ML spacers. The dotted lines marking the PLE resonances are only guides to the eye. For the single-layer sample the two excitation resonances are found invariably at  $\Delta E_1 = 71.4$  and  $\Delta E_2 = 103.8$  meV, whereas for the two-layer and the 1.138-eV peak of the five-layer sample  $\Delta E_1$  and  $\Delta E_2$  decrease with decreasing ground-state transition energy. This behavior reflects the decreasing excited-state splitting in QD's of increasing size. The FWHM of the PLE resonances probing a QD ensemble is large ( $\sim 25$  meV) in contrast to sharp lines observed for single QD's.<sup>44</sup> PLE overcomes the inhomogeneous broadening of the *ground-state* transition of the QD ensemble by setting a narrow detection window centered at  $E_{\text{det}}$ , and probes the inhomogeneously broadened *excited-state* spectrum of this subset. The inhomogeneity of the self-assembled QD's, either in a single set or within the stacked layers, is not restricted to volume variations alone, but also involves the shape of the islands. Thus, even for a defined ground-state transition energy, the excited-state spectrum will be inhomogeneously broadened, and the FWHM of the PLE resonances is a measure for the shape nonuniformity. The high excitation density PL spectra of the multilayered samples show the first excited-state transition between 80 and 100 meV above the ground-state transition in good agreement with the dominating resonance in the better resolved PLE spectra.

Figure 5 summarizes the energy shift  $\Delta E$  of the PLE resonances with respect to the detection energy for the multilayered samples with 36-ML spacers. Plan view and cross-sectional transmission electron microscopy (TEM) investigations of the *single-layer* sample as well as of an identical but uncapped sample are consistent with a pyramidal shape of the islands, with a base length of  $(12 \pm 2)$  nm and predominantly  $\{302\}$  type side facets.<sup>45</sup> The QD shape and base length are similar to other observations for different growth conditions.<sup>5,46</sup> Calculations for pyramidal QD's with  $\{101\}$  (Ref. 17) and  $\{302\}$  (Ref. 19) side facets give only a single localized electron state and locate the first excited  $|001\rangle$ ,  $|010\rangle$ , and  $|100\rangle$  hole states about 60–110 meV

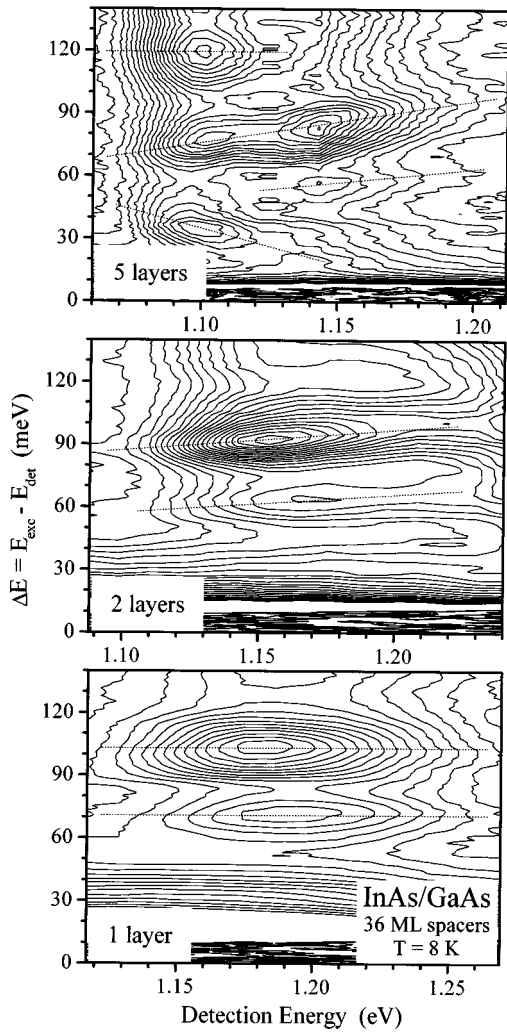


FIG. 4. Contour plots of the QD PL intensity as a function of the detection energy and the excess excitation energy  $\Delta E = E_{\text{exc}} - E_{\text{det}}$  for multilayered samples with 36-ML spacers. The dotted lines are only guides to the eye following the PLE resonances marked by arrows in Fig. 3.

above the  $|000\rangle$  ground state depending on the QD size and shape. Thus, the dominant excitation resonance observed 60–103 meV above the detection energy might be attributed to the transition between the electron ground state and an excited hole state, most likely the  $|001\rangle$  hole state, which has a larger oscillator strength than transitions involving the  $|010\rangle$  and the  $|100\rangle$  hole levels.<sup>17</sup> This assignment is in agreement with that of excited-state transitions observed in high excitation density PL experiments<sup>19</sup> and supported by the observation of multi-LO-phonon replicas in the QD PLE spectra<sup>27</sup> as well as the Zeeman behavior.<sup>47</sup> The PLE results shown in Figs. 4 and 5 give, for the first time, experimental evidence for the expected volume dependence of the excited-state spectrum of self-assembled QD's.

Widely varying shapes have been reported for self-assembled InAs islands in single-layer samples,<sup>3–7,19</sup> indicating that the thermodynamic equilibrium shape of the islands ( $\{101\}$  side facets)<sup>48</sup> is generally not achieved in the kinetically limited formation process, but that the islands have a tendency to form shallower side facets. Additionally, for

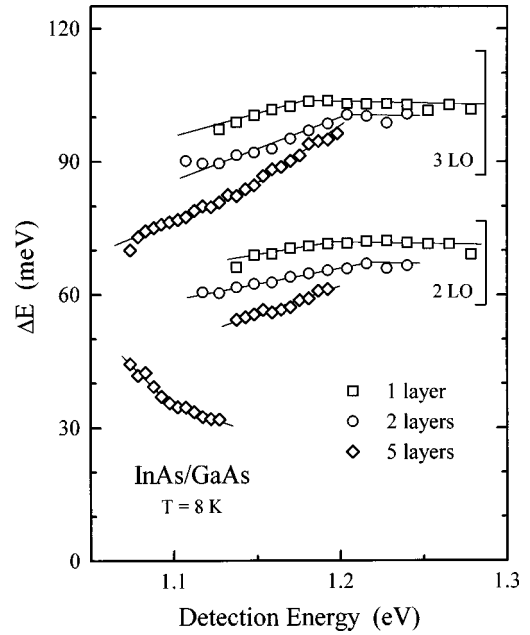


FIG. 5. The excess excitation energy  $\Delta E = E_{\text{exc}} - E_{\text{det}}$  of QD PLE resonances observed for multilayered InAs/GaAs samples with 36-ML spacers. The energy ranges for the excited-state splitting allowing efficient multiphonon relaxation (two or three LO phonons) are marked.

single-layer samples a trend for larger volume islands to have flatter side facets has been inferred from optical results.<sup>19,27</sup> Figures 4 and 5 evidence a pronounced effect of the vertical stacking of InAs islands on the observed PLE spectra. With increasing number of InAs layers the PLE resonances shift for the same ground-state transition energy towards lower energies and the low-energy shift of the resonances with the decreasing ground-state transition energy becomes steeper. We propose this behavior to indicate a systematic change of the InAs island shape in the stacking process as illustrated in Fig. 6, namely, an increasing height-to-width aspect ratio and an improving shape uniformity of the islands in the higher layers. TEM images of uncapped islands in a single layer sample with 1.74-ML InAs deposition show side facets close to  $\{302\}$ .<sup>45</sup> The PLE results suggest that the islands in the higher layers become steeper in

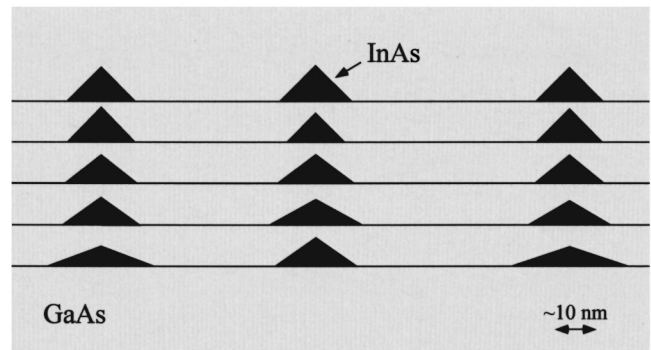


FIG. 6. Schematic illustrating the evolution of the InAs island size and shape in multilayered samples. The height-to-width aspect ratio increases and the shape uniformity improves for islands in the upper layers.

the stacking process. However, this effect is not easily resolved in cross-sectional TEM images of stacked samples, where strain contrast masks changes in the island shape as, e.g., in Fig. 1(c) of Ref. 31 for the five-layer sample with 36-ML spacers. The decreasing intensity of the 60-meV resonance compared to that of the 100-meV resonance with increasing number of layers (lowest three spectra in Fig. 3) is attributed to the narrowing of the inhomogeneous excited-state splitting and supports an improving shape uniformity. We propose a systematic change in island shape to be intricately bound to the vertical self-organization of the islands in the stacked samples. It is now well established<sup>31,34</sup> that vertical self-organization is a consequence of the contribution of buried InAs islands to the surface strain distribution dictating the surface migration of In in the second layers.<sup>31</sup>

The PLE spectra dominated by a narrow resonance around  $\Delta E = 100$  meV discussed up to now are characteristic for electronically *uncoupled* QD's. However, the increasing island height in the upper layers reduces the GaAs barrier between the stacked islands and might eventually lead to electronic coupling. The 1.099-eV peak (Fig. 1) dominating the PL of the five-layer sample with 36-ML spacers for low-density GaAs excitation is attributed to such *coupled* QD's. The contour plot of the PL intensity of the five-layer sample in Fig. 4 shows a different behavior (marked by dashed lines in Fig. 4) for the 1.138- and 1.099-eV peaks. The intensity of the 100-meV resonance attributed to the  $|001\rangle_h|000\rangle_e$  excited state absorption of uncoupled QD's is shown in Fig. 2(b) as a function of the detection energy, demonstrating the correlation with the 1.138-eV peak. For the 1.099-eV peak two additional excitation resonances at about 35 and 120 meV are observed. The 35-meV resonance is too broad and intense to be attributed to Raman scattering and shifts towards higher energies with decreasing detection energy (see Fig. 5). A stronger electronic coupling for larger and therefore higher QD's, which result in a thinner GaAs barrier between the stacked QD's, could explain this behavior. For thinner spacers (20 ML) the PLE spectrum shows only weak structure peaking about 60 meV above the detection energy (dashed spectrum in Fig. 3). This behavior is characteristic of strongly coupled QD's.<sup>42</sup> Higher-resolution PLE spectra resolving fine structure in the energy range below 30 meV would be needed for a detailed analysis of the electronic coupling in the QD stacks. However, the results presented here demonstrate the inequivalence of the various InAs layers in the multilayered samples.

#### IV. CARRIER CAPTURE, RELAXATION, AND RECOMBINATION

The observation of excited state resonances in the PLE spectra of single and multilayer InAs/GaAs self-assembled QD's discussed above is in striking contrast to the observation of multiphonon resonances for single-layer samples examined in Refs. 13, 14, 27, and 43. Distinct replica corresponding to multiphonon scattering involving LO phonons from the InAs QD, the WL and the GaAs barrier have been resolved,<sup>13,27</sup> demonstrating inelastic multiphonon scattering to be the most efficient intradot carrier relaxation process. The observation of the multiphonon resonances has been explained in analogy to hot carrier relaxation in higher-

dimensional systems,<sup>49</sup> which leads to multiple LO resonances in PLE spectra, when competing nonradiative recombination allows only the most efficient relaxation processes (LO scattering) to populate the luminescent state. For QD's having a discrete density of states the inhomogeneous broadening of the ensemble replaces the spatial dispersion in higher-dimensional systems. For self-assembled InAs/GaAs QD's radiative recombination<sup>43</sup> as well as a nonradiative recombination involving deep defects in the barrier<sup>13,27</sup> have been proposed to compete with intradot relaxation. In both cases only QD's providing rapid carrier relaxation will contribute to the PLE signal, and the observed multiphonon resonances demonstrate a resonance condition for the excited-state splitting. The observation of excited-state resonances reported in this paper (Figs. 4 and 5) shows the lack of an efficient competing recombination channel in the investigated samples. Indeed, the maximum of the excitation via the  $|001\rangle$  hole state is observed for an excited state splitting of 83 meV (five-layer sample, Fig. 4) for which multiphonon relaxation is inefficient.<sup>27</sup> These results demonstrate the extrinsic nature of any competing recombination channel for InAs/GaAs QD's, thus supporting the earlier notion of nonradiative energy transfer to deep defects in the GaAs barrier for samples showing clear multiphonon resonances.<sup>27</sup> We attribute the lower defect concentration in the GaAs barriers of the present samples to the employed MEE growth mode, which has been observed to improve the QD PL yield.<sup>6</sup> In order to gain insight into the carrier relaxation and recombination dynamics in the stacked InAs/GaAs QD samples we have investigated the dynamic behavior of the QD PL following pulsed excitation with various energies and densities.

In TRPL experiments the suppression of intra-dot carrier relaxation due to saturation of QD states results in characteristic changes in the observed PL dynamics.<sup>27,50,51</sup> For the self-assembled InAs/GaAs QD's carrier relaxation ( $\sim 40$  ps) (Ref. 27) is much faster than radiative recombination. Thus, carriers generated by the short excitation pulse (150 fs) will fill up QD levels starting from the ground state after an initial capture and relaxation phase, which might be dominated by Coulomb scattering.<sup>51</sup> With increasing delay the hole density decreases due to carrier recombination and the various QD states will be successively depopulated. The PL intensity from a given state being proportional to its population remains almost constant as long as higher-lying states are populated providing practically instantaneous holes to fill up freed states. Only the PL intensity from the highest populated state decays with a time constant corresponding to the sum of the radiative recombination probability and the rate at which recombination generates a lower-lying empty state enabling intradot relaxation. This will lead to systematically shorter decay times for PL from higher excited states though the oscillator strength might actually be lower than for the ground-state transition. Master equations for microstates (MEM) provide a quantitative description of the PL dynamics for uncoupled QD's as detailed in reference.<sup>52</sup>

Figure 7 compares PL spectra of the five-layer sample with 20-ML spacers for continuous-wave (cw) and pulsed excitation revealing excited-state PL with increasing excitation density. For high intensity cw excitation the excited-state PL intensity is comparable to the ground-state intensity

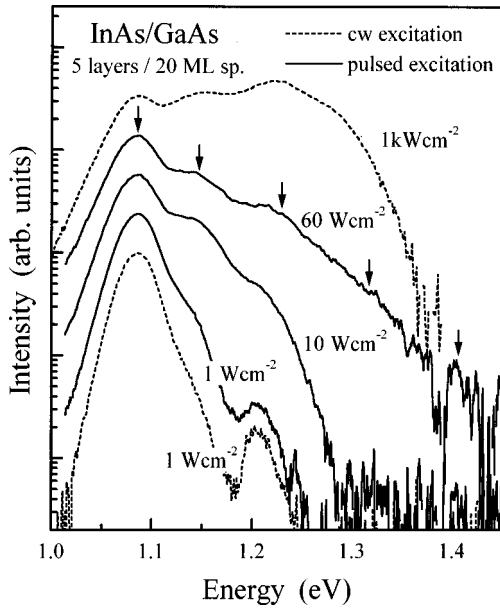


FIG. 7. Excitation density dependence of the QD PL in the five-layer sample with 20-ML spacers for cw (dashed spectra) and pulsed (solid spectra) excitation. The spectra are normalized for the QD ground-state transition and shifted in the  $y$  direction for clarity. The given excitation densities are time averaged, with  $1 \text{ W cm}^{-2}$  corresponding for pulsed excitation to an initial carrier density of about  $2 \times 10^{10} \text{ cm}^{-2}$  comparable to the lateral QD density.

indicating comparable oscillator strength, whereas for pulsed excitation the subsequent depopulation of excited states results in a lower integrated intensity for the excited-state transitions. However, the same time-averaged excitation density provides initially a higher carrier density for pulsed excitation. The lowest excitation density of  $1 \text{ W cm}^{-2}$  is already sufficient to saturate the ground state of part of the QD's. At  $10 \text{ W cm}^{-2}$  the first excited state is saturated and the second one becomes populated. At  $60 \text{ W cm}^{-2}$  PL appears in the spectral region of the WL indicating the QD states to be completely saturated. Figure 8 gives transients recorded at the positions (indicated by arrows in Fig. 7) of the ground-state and various excited-state transitions showing the expected initially almost constant intensity as long as PL from higher-energy states is observed. The PL intensity, however, is initially not perfectly constant as a result of a laterally inhomogeneous excitation density, carrier diffusion, and the statistical population of the uncoupled QD's after nonresonant excitation.<sup>52</sup> Multiexponential fits of the excited-state PL transients yield a decay time of about 480 ps for PL from the first excited state, which decreases to 15 ps for PL above 1.4 eV attributed to exciton recombination in the WL, reflecting the increasing number of recombination channels with increasing population of the QD's. A fit of the PL transients, recorded at  $1 \text{ W cm}^{-2}$ , using MEM yields lifetimes of 0.95 and 1.55 ns for the ground and first excited-state transition, respectively. The long excited-state lifetime is compatible with the forbidden character of the  $|001\rangle_h|000\rangle_e$  transition.

The high excitation density PL transients, Fig. 8, show saturation of the ground-state transition for up to 1 ns after the initial excitation, and the first and second excited states remain saturated for a few hundred ps. This behavior is in

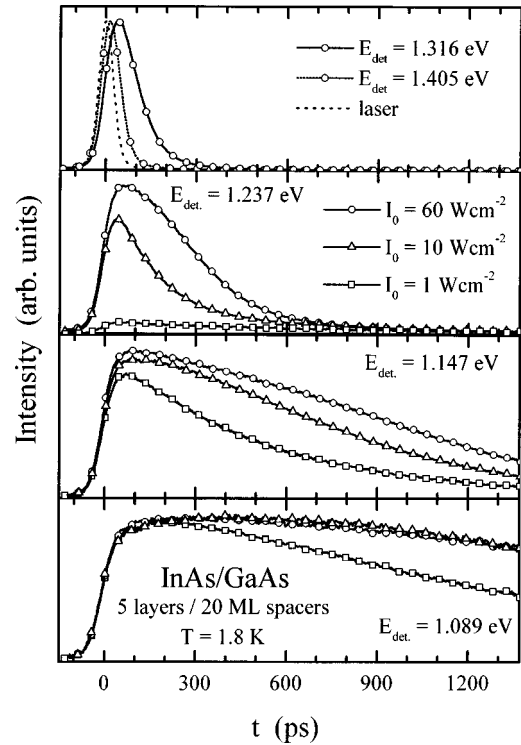


FIG. 8. Transients recorded at various excitation densities for the five-layer sample with 20-ML spacers at the spectral positions corresponding to PL from the ground state and various excited states as indicated by arrows in Fig. 7. The transients are normalized for the slow decay component attributed to the underlying ground-state decay of smaller QD's.

contrast to the earlier observation of very rapid excited-state PL decay ( $< 100 \text{ ps}$ ) at high excitation densities, which has been taken as indication of nonradiative recombination.<sup>27</sup> The long-lived excited-state PL in the present samples suggests radiative recombination to dominate for the excited QD states, demonstrating the high optical quality of the investigated samples. The MEE growth technique used for the GaAs spacer and the cap layers provides GaAs with low defect concentrations at the growth temperature of  $400 \text{ }^\circ\text{C}$ . The importance of the GaAs cap growth mode was manifest in the increase in PL efficiency for samples with the cap layer grown in the MEE mode compared to those grown with conventional MBE.<sup>6</sup>

Pauli blocking can be neglected at low excitation densities ( $\leq 0.5 \text{ W cm}^{-2}$ ), in which case the transients are generally well fitted assuming one exponential rise and one exponential decay process, describing carrier relaxation and recombination in a three-level system. The uppermost level is populated at  $t=0$  and relaxes with rate  $\tau_1^{-1}$  to the luminescent level, before recombination into the ground state occurs with rate  $\tau_2^{-1}$ . The shorter of the two time constants determines the rise and the longer one governs the decay of the time-dependent PL intensity  $I$ :

$$I(t) \propto \frac{1}{\tau_1 - \tau_2} (\exp^{-t/\tau_1} - \exp^{-t/\tau_2}). \quad (1)$$

Figure 9 shows a typical low excitation density QD PL transient (dots) for the case of the two InAs-layer sample

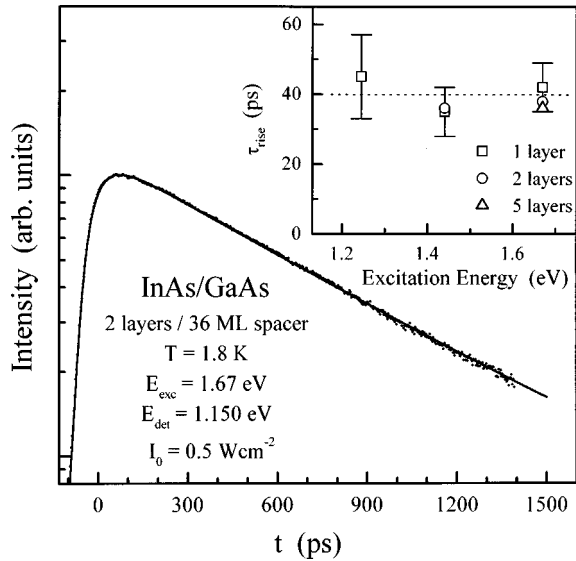


FIG. 9. Transient of the QD PL in the two-layer sample with 36-ML spacer for nonresonant, low-density ( $0.5 \text{ W cm}^{-2}$ ) excitation in the GaAs barrier. Dots represent the experimental data and the full line shows a two-exponential fit as described in the text. The inset shows the rise time ( $\tau_{\text{rise}}$ ) of the QD PL maximum in multilayered samples with 36-ML spacers for various excitation energies. The error bars given for the single layer sample are also representative for the stacked ones.

with a 36-ML spacer together with a least-square fit (full line) of the convolution of Eq. (1) with the system response to the exciting laser pulses. Evaluating transients of multilayered samples with 36-ML spacers we find time constants of about 40 ps for the PL rise and of a few hundred ps for the PL decay, which are summarized in Fig. 10. Nonresonant excitation of the GaAs barrier generates free electron-hole pairs, which have to diffuse or migrate to the QD's, before

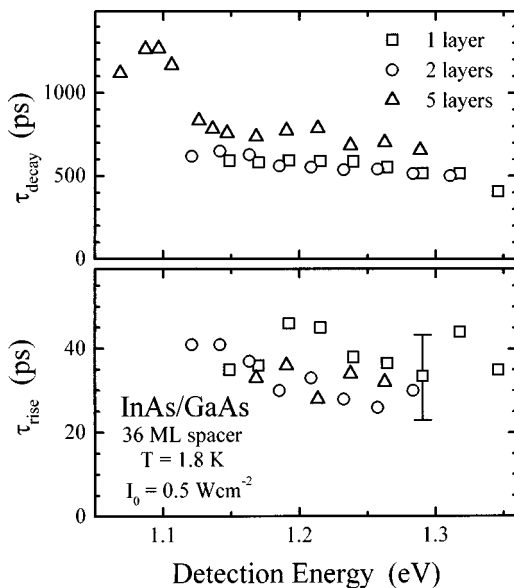


FIG. 10. QD PL rise ( $\tau_{\text{rise}}$ ) and decay ( $\tau_{\text{decay}}$ ) times as a function of the detection energy for multilayered samples with 36-ML spacers upon nonresonant, low-density excitation in the GaAs barrier. The experimental error of the rise (decay) time is about 10 ps (70 ps).

they can be captured into a localized state and relax by interlevel scattering to the QD ground state, leading to the PL detected in our experiments. The lack of free exciton PL from the GaAs barrier and the InAs WL as well as the lack of excited-state PL at low excitation densities indicate the observed 40-ps rise time to describe carrier capture and relaxation and the longer time constant to describe ground-state recombination. Both the rise and the decay times (Fig. 10) vary only weakly with the detection energy as well as the number of stacks in the sample. These findings suggest the oscillator strength to be practically independent of the QD size, supporting the prediction of a constant interband oscillator strength in the strong confinement regime.<sup>53,54</sup> The observed lifetimes are, however, shorter than those reported previously.<sup>9,27,55</sup> More detailed investigations are necessary to evaluate the size and shape dependence of the transition matrix element. Remarkably, the TRPL results show for the five-layer sample a sharp increase in the PL decay time below 1.12 eV. PL in this region is attributed to coupled QD's, suggesting a decreasing oscillator strength for weakly coupled QD's. An increasing oscillator strength with decreasing barrier thickness has been reported for strongly coupled QD's.<sup>11</sup>

TRPL measurements for various excitation energies allow a more detailed characterization of the excitation dynamics. Although for excitation near the hh transition of the WL (1.44 eV) or via excited state transitions of the QD's (1.25 eV) carrier diffusion and carrier capture into excited states, respectively, are excluded from the excitation chain, the transients, within the experimental error, are the same as for excitation in the GaAs barrier. As shown in the inset of Fig. 9, the observed PL rise time is  $(40 \pm 5)$  ps independent of the chosen excitation energy/process as well as the number of stacks in the sample and thus limited by intradot relaxation processes. The observed PL rise time is in good agreement with recent experimental results on single-layer samples<sup>27,30</sup> and attributed to multiphonon relaxation of the excited hole states.

The TRPL results yield only an upper limit ( $< 5$  ps) for capture into excited QD states. However, the PLE results give indirect evidence for sub-ps carrier capture inferred earlier from the quantum efficiency of deep etched mesa structures.<sup>56</sup> Figure 11 shows the PLE behavior of the QD ground-state PL for the two-layer sample. The excitation efficiency in the GaAs barrier shows minima separated by  $(43 \pm 2)$  meV that extrapolate to the free-exciton (FE) energy as indicated. The observed energy spacing  $\Delta E$  is characteristic for hot-electron relaxation in GaAs, given by<sup>49</sup>

$$\Delta E = \hbar \omega_{\text{LO}} \times \left( 1 + \frac{m_e}{m_h} \right) = 41.4 \text{ meV}, \quad (2)$$

with  $\hbar \omega_{\text{LO}}$  the LO phonon energy and  $m_i$  the effective masses of electrons and holes. An energy spacing of 41.4 meV is expected from GaAs parameters. The observation of hot-electron relaxation leading to minima in the PLE efficiency indicates the formation of low-mobility FE's near the  $\Gamma$  point to compete with carrier trapping into QD's. For this competition to be observable in the PLE spectra, both processes have to proceed on a comparable time scale locating carrier capture on a subpicosecond time scale. Exciton local-

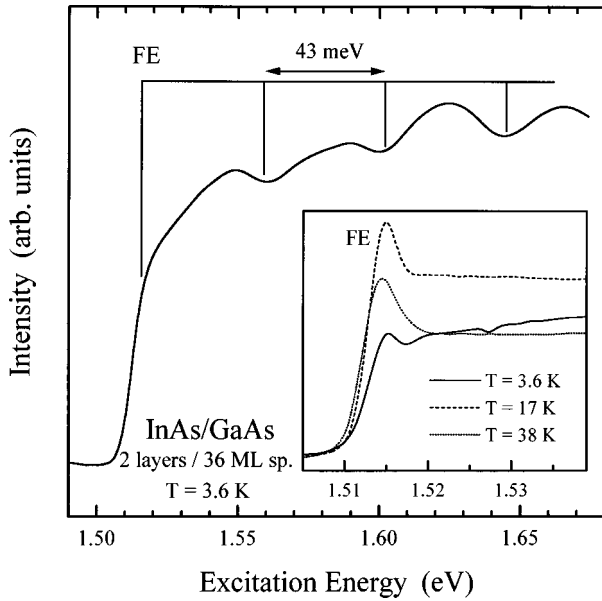


FIG. 11. PLE spectrum of the QD PL (detected at 1.159 eV) in the two-layer sample with 36-ML spacer. The minima in the PLE efficiency are attributed to hot-electron relaxation in the GaAs barrier. The inset shows the GaAs band-gap region on an enlarged energy scale for various temperatures.

ization in the GaAs barrier hampering QD excitation is also revealed by the temperature dependence of the PLE spectra, inset of Fig. 11. At 3.6 K the GaAs FE absorption is practically not resolved and the PLE spectra reveal the hot-electron relaxation minima. Raising the temperature to 17 K, the FE absorption appears and the PLE efficiency becomes smooth at higher energies attributed to the thermally activated mobility of FE's.

PLE spectra taken for various temperatures at the peak of the QD PL in the two-layer sample reveal remarkable differences in the intensity evolution depending on the excitation process. Figure 12 depicts the intensity of the QD ground-state PL for excitation in the GaAs barrier, the hh transition of the WL, and the  $|001\rangle_h|000\rangle_e$  excited-state transition resonance as indicated in the inset. Exciting the GaAs barrier (triangles) the PL intensity doubles from 4 to 18 K only to decrease again with increase of temperature to 35 K, showing the increasing mobility of the FE's and their thermal dissociation, respectively. The FE effect is absent when exciting via the WL. The decrease of the PL intensity above 80 K observed for nonresonant excitation has been attributed to thermal evaporation of carriers from the ground state.<sup>9,55,57</sup> However, exciting carriers directly into the  $|001\rangle_h$  excited hole state of the QD's (circles) leads to a significantly higher-temperature stability of the PL intensity. These results show that actually the carrier capture and relaxation processes determine the observed temperature dependence of the QD PL intensity for nonresonant excitation. The decreasing capture efficiency above 80 K, is attributed to a decreasing carrier capture efficiency due to thermal evaporation of carriers from excited QD states.

## V. CONCLUSION

In the present paper the effect of stacking on the excited states and carrier relaxation processes of InAs QD's is inves-

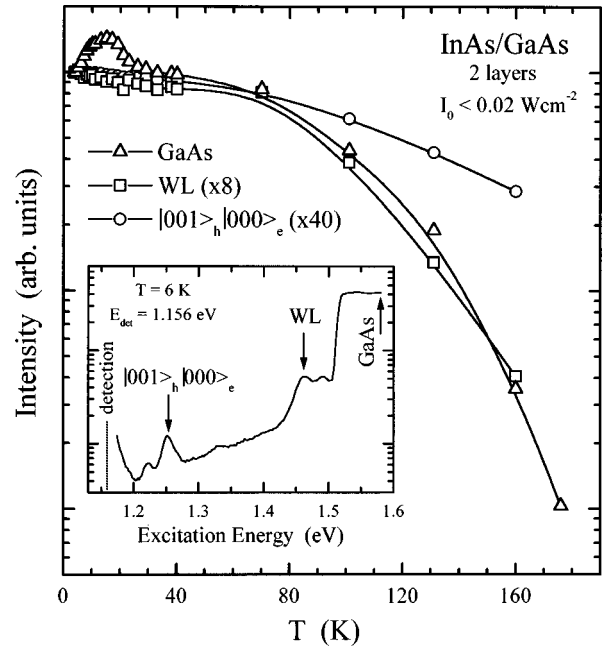


FIG. 12. Temperature dependence of the QD PL intensity in the two-layer sample with 36-ML spacer for excitation in the GaAs barrier, in the InAs WL, and via the excited  $|001\rangle_h|000\rangle_e$  hole state. The intensities are evaluated from PLE spectra detected at the maximum of the temperature-dependent QD PL peak as indicated in the inset.

tigated using PLE and TRPL spectroscopy. The contribution of the buried InAs islands to the surface strain directing the In migration leads not only to vertical ordering of the islands but, as suggested by the results presented, also to an increasingly higher degree of island uniformity. The optical results demonstrate unambiguously the inequivalence of the various InAs QD layers for samples with 36-ML GaAs spacers, indicating a systematic variation of the island shape in the stacks. The ground-state transition energy of the stacked QD's is found to decrease compared to that of isolated QD's as a result of the higher degree of strain relaxation and electronic coupling. The systematic change in island shape complicates control of the electronic coupling in the QD stacks.

PLE spectra reveal the size-dependence of the excited-state spectrum for self-assembled InAs QD's. The dominant excitation resonance is attributed to the  $|001\rangle_h|000\rangle_e$  excited state transition based on numerical results for pyramidal InAs islands, supporting the earlier assignment of the excited-state transitions observed in high excitation density PL to transitions between excited hole states and the electron ground state.<sup>19</sup> State-filling effects are found to dominate the PL dynamics in densely populated QD's for up to 1 ns, attributed to a low concentration of competing nonradiative recombination channels in the investigated samples due to the MEE growth of the GaAs spacer and cap layers. Carrier capture and intradot carrier relaxation lead to a  $(40 \pm 5)$  ps rise time for the QD ground-state PL, attributed to multiphonon relaxation of the  $|001\rangle_h$  hole state. Carrier cooling is about two orders of magnitude slower than in higher-dimensional systems but still over one order of magnitude faster than radiative recombination, explaining the apparent lack of a phonon bottleneck in PL experiments. However,

carrier relaxation is found to limit the PL yield at temperatures above 80 K and might lead to a bottleneck effect in the stimulated emission regime, limiting the high-frequency behavior of QD injection lasers and causing lasing on excited state transitions depending on the gain/loss balance.

## ACKNOWLEDGMENTS

Parts of this work were supported by the U.S. Air Force Office of Scientific Research and by the Deutsche Forschungsgemeinschaft in the framework of Sonderforschungsbereich 296.

- <sup>1</sup>S. Guha, A. Madhukar, and K. C. Rajkumar, *Appl. Phys. Lett.* **57**, 2110 (1990).
- <sup>2</sup>D. J. Eaglesham and M. Cerullo, *Phys. Rev. Lett.* **64**, 1943 (1990).
- <sup>3</sup>D. Leonard, K. Pond, and P. M. Petroff, *Phys. Rev. B* **50**, 11 687 (1994).
- <sup>4</sup>J. M. Moison, F. Houzay, F. Barthe, L. Leprince, E. Andre, and O. Vatel, *Appl. Phys. Lett.* **64**, 196 (1994).
- <sup>5</sup>M. Grundmann, N. N. Ledentsov, R. Heitz, L. Eckey, J. Christen, J. Böhrer, D. Bimberg, S. S. Ruvimov, P. Werner, U. Richter, J. Heydenreich, V. M. Ustinov, A. Yu. Egorov, A. E. Zhukov, P. S. Kop'ev, and Zh. I. Alferov, *Phys. Status Solidi B* **188**, 249 (1995).
- <sup>6</sup>Q. Xie, P. Chen, A. Kalburge, T. R. Ramachandran, A. Nayfonov, A. Konkar, and A. Madhukar, *J. Cryst. Growth* **150**, 357 (1995).
- <sup>7</sup>N. P. Kobayashi, T. R. Ramachandran, P. Chen, and A. Madhukar, *Appl. Phys. Lett.* **68**, 3299 (1996).
- <sup>8</sup>See, for example, *Strained-Layer Superlattices: Physics*, edited by T. Pearsall, *Semiconductors and Semimetals Vol. 32* (Academic, New York, 1990); *Strained-Layer Superlattices: Materials Science and Technology*, edited by T. P. Pearsall, *Semiconductors and Semimetals Vol. 33* (Academic, Boston, 1991).
- <sup>9</sup>N. Kirstaedter, N. N. Ledentsov, M. Grundmann, D. Bimberg, U. Richter, S. S. Ruvimov, P. Werner, J. Heydenreich, V. M. Ustinov, M. V. Maximov, P. S. Kop'ev, and Zh. I. Alferov, *Electron. Lett.* **30**, 1416 (1994); D. Bimberg, N. N. Ledentsov, M. Grundmann, N. Kirstaedter, O. Schmidt, V. M. Ustinov, A. Yu. Egorov, A. E. Zhukov, P. S. Kop'ev, Zh. I. Alferov, S. S. Ruvimov, U. Gösele, and J. Heydenreich, *Jpn. J. Appl. Phys., Part 1* **35**, 1311 (1996).
- <sup>10</sup>Q. Xie, A. Kalburge, P. Chen, and A. Madhukar, *IEEE Photonics Technol. Lett.* **8**, 965 (1996).
- <sup>11</sup>N. N. Ledentsov, V. A. Shchukin, M. Grundmann, N. Kirstaedter, J. Böhrer, O. Schmidt, D. Bimberg, V. M. Ustinov, A. Y. Egorov, A. E. Zhukov, P. S. Kop'ev, S. V. Zaitsev, N. Yu. Gordeev, Z. I. Alferov, A. I. Borovkov, A. O. Kosogov, S. S. Ruvimov, P. Werner, U. Gösele, and J. Heydenreich, *Phys. Rev. B* **54**, 8743 (1996).
- <sup>12</sup>Y. Arakawa and S. Sakaki, *Appl. Phys. Lett.* **40**, 939 (1982).
- <sup>13</sup>R. Heitz, M. Grundmann, N. N. Ledentsov, L. Eckey, M. Veit, D. Bimberg, V. M. Ustinov, A. Yu. Egorov, A. E. Zhukov, P. S. Kop'ev, and Zh. I. Alferov, *Appl. Phys. Lett.* **68**, 361 (1996).
- <sup>14</sup>K. H. Schmidt, G. Medeiros-Ribeiro, M. Oestereich, P. M. Petroff, and G. H. Döhler, *Phys. Rev. B* **54**, 11 346 (1996).
- <sup>15</sup>A. Wojs, P. Hawrylak, S. Fafard, and L. Jacak, *Phys. Rev. B* **54**, 5604 (1996).
- <sup>16</sup>K. Mukai, N. Ohtsuka, H. Shoji, and M. Sugawara, *Phys. Rev. B* **54**, R5243 (1996).
- <sup>17</sup>M. Grundmann, O. Stier, and D. Bimberg, *Phys. Rev. B* **52**, 11 969 (1995).
- <sup>18</sup>M. A. Cusack, P. R. Briddon, and M. Jaros, *Phys. Rev. B* **54**, R2300 (1996).
- <sup>19</sup>M. Grundmann, N. N. Ledentsov, O. Stier, J. Böhrer, D. Bimberg, V. M. Ustinov, P. S. Kop'ev, and Zh. I. Alferov, *Phys. Rev. B* **53**, R10 509 (1996).
- <sup>20</sup>S. Fafard, R. Leon, D. Leonard, J. L. Merz, and P. M. Petroff, *Phys. Rev. B* **52**, 5752 (1995).
- <sup>21</sup>H. Lipsanen, M. Sopanen, and J. Ahopelto, *Phys. Rev. B* **51**, 13 868 (1995).
- <sup>22</sup>K. Mukai, N. Ohtsuka, H. Shoji, and M. Sugawara, *Appl. Phys. Lett.* **68**, 3013 (1996).
- <sup>23</sup>H. Drexler, D. Leonard, W. Hansen, J. P. Kotthaus, and P. M. Petroff, *Phys. Rev. Lett.* **73**, 2252 (1994).
- <sup>24</sup>K. Brunner, G. Abstreiter, G. Böhm, G. Tränkle, and G. Weimann, *Phys. Rev. Lett.* **73**, 1138 (1994).
- <sup>25</sup>G. Medeiros-Ribeiro, F. G. Pikus, P. M. Petroff, and A. L. Efros, *Phys. Rev. B* **55**, 1568 (1997).
- <sup>26</sup>M. Grundmann, J. Christen, N. N. Ledentsov, J. Böhrer, D. Bimberg, S. S. Ruvimov, P. Werner, U. Richter, U. Gösele, J. Heydenreich, V. M. Ustinov, A. Yu. Egorov, A. E. Zhukov, P. S. Kop'ev, and Zh. I. Alferov, *Phys. Rev. Lett.* **74**, 4043 (1995).
- <sup>27</sup>R. Heitz, M. Veit, N. N. Ledentsov, A. Hoffmann, D. Bimberg, V. M. Ustinov, P. S. Kop'ev, and Zh. I. Alferov, *Phys. Rev. B* **56**, 10 435 (1997).
- <sup>28</sup>H. Benisty, C. M. Sotomayor-Torres, and C. Weisbuch, *Phys. Rev. B* **44**, 10 945 (1991).
- <sup>29</sup>T. Inoshita and H. Sakaki, *Phys. Rev. B* **46**, 7260 (1992).
- <sup>30</sup>B. Ohnesorge, M. Albrecht, J. Oshinowo, A. Forchel, and Y. Arakawa, *Phys. Rev. B* **54**, 11 532 (1996).
- <sup>31</sup>Q. Xie, A. Madhukar, P. Chen, and N. P. Kobayashi, *Phys. Rev. Lett.* **75**, 2542 (1995).
- <sup>32</sup>A. Madhukar, P. Chen, Q. Xie, A. Konkar, T. R. Ramachandran, N. P. Kobayashi, and R. Viswanathan, in *Low Dimensional Structures prepared by Epitaxial Growth or Regrowth on Patterned Substrates*, edited by K. Eberl, P. Demecster, and P. Petroff (Kluwer Academic, The Netherlands, 1995), p. 19.
- <sup>33</sup>L. Goldstein, F. Glas, J. Y. Marzin, M. N. Charasse, and G. Le Roux, *Appl. Phys. Lett.* **47**, 1099 (1985).
- <sup>34</sup>G. S. Solomon, J. A. Trezza, A. F. Marshall, and J. S. Harris, *Phys. Rev. Lett.* **76**, 952 (1996).
- <sup>35</sup>J. Tersoff, C. Teichert, and M. G. Lagally, *Phys. Rev. Lett.* **76**, 1675 (1996).
- <sup>36</sup>C. Teichert, M. G. Lagally, L. J. Peticolas, J. C. Bean, and J. Tersoff, *Phys. Rev. B* **53**, 16 334 (1996).
- <sup>37</sup>Q. Xie, N. P. Kobayashi, T. R. Ramachandran, A. Kalburge, P. Chen, and A. Madhukar, *J. Vac. Sci. Technol. B* **14**, 2203 (1996).
- <sup>38</sup>T. R. Ramachandran, R. Heitz, P. Chen, and A. Madhukar, *Appl. Phys. Lett.* **70**, 640 (1997).
- <sup>39</sup>R. Heitz, T. R. Ramachandran, A. Kalburge, Q. Xie, I.

- Mukhametzhanov, P. Chen, and A. Madhukar, *Phys. Rev. Lett.* **78**, 4071 (1997).
- <sup>40</sup>M. Ilg, M. I. Alonso, A. Lehmann, K. H. Ploog, M. Hohenstein, J. Appl. Phys. **74**, 7188 (1993).
- <sup>41</sup>P. D. Wang, N. N. Ledentsov, C. M. Sotomayor-Torres, I. N. Yassievich, A. Pakhomov, A. Yu. Egorov, P. S. Kop'ev, and V. M. Ustinov, *Phys. Rev. B* **50**, 1604 (1994).
- <sup>42</sup>M. Grundmann, N. N. Ledentsov, R. Heitz, D. Bimberg, V. M. Ustinov, A. Yu. Egorov, M. V. Maximov, P. S. Kop'ev, and Zh. I. Alferov, S. S. Ruminov, P. Werner, J. Heydenreich, and U. Gösele, *Proceedings of the 8th International Conference on InP and Related Materials* (IEEE, Schwäbisch Gmünd, 1996), p. 738.
- <sup>43</sup>M. J. Steer, D. J. Mowbray, W. R. Tribe, M. S. Skolnick, M. D. Sturge, M. Hopkinson, A. G. Cullis, C. R. Whitehouse, and R. Murray, *Phys. Rev. B* **54**, 17 738 (1997).
- <sup>44</sup>M. Notomi, T. Furuta, H. Kamada, J. Temmyo, and T. Tamamura, *Phys. Rev. B* **53**, 15 743 (1996).
- <sup>45</sup>Q. Xie, Ph.D. Dissertation, University of Southern California, 1997.
- <sup>46</sup>S. Ruvimov, P. Werner, K. Scheerschmidt, J. Heydenreich, U. Richter, N. N. Ledentsov, M. Grundmann, D. Bimberg, V. M. Ustinov, A. Yu. Egorov, P. S. Kop'ev, and Zh. I. Alferov, *Phys. Rev. B* **51**, 14 766 (1995).
- <sup>47</sup>L. R. Wilson, D. J. Mowbray, M. S. Skolnick, M. Morifuji, M. J. Steer, I. A. Larkin, and M. Hopkinson, *Phys. Rev. B* **57**, R2073 (1998).
- <sup>48</sup>V. A. Shchukin, N. N. Ledentsov, P. S. Kop'ev, and D. Bimberg, *Phys. Rev. Lett.* **75**, 2968 (1995).
- <sup>49</sup>S. A. Permogorov, *Phys. Status Solidi B* **68**, 9 (1975).
- <sup>50</sup>P. Castrillo, D. Hessman, M.-E. Pistol, S. Anand, N. Carlsson, W. Seifert, and L. Samuelson, *Appl. Phys. Lett.* **67**, 1905 (1995).
- <sup>51</sup>S. Grosse, J. H. H. Sandmann, G. Von Plessen, J. Feldmann, H. Lipsanen, M. Sopanen, J. Tulkki, and J. Ahopelto, *Phys. Rev. B* **55**, 4473 (1997).
- <sup>52</sup>M. Grundmann and D. Bimberg, *Phys. Rev. B* **55**, 9740 (1997).
- <sup>53</sup>E. Hanamura, *Phys. Rev. B* **37**, 1273 (1988).
- <sup>54</sup>M. Sugawara, *Phys. Rev. B* **51**, 10 743 (1995).
- <sup>55</sup>G. Wang, S. Fafard, D. Leonard, J. E. Bowers, J. L. Merz, and P. M. Petroff, *Appl. Phys. Lett.* **64**, 2815 (1994).
- <sup>56</sup>N. N. Ledentsov, M. V. Maximov, P. S. Kop'ev, V. M. Ustinov, M. V. Belousov, B. Ya. Meltser, S. V. Ivanov, V. A. Shchukin, Zh. I. Alferov, M. Grundmann, D. Bimberg, S. S. Ruvimov, W. Richter, P. Werner, U. Gösele, J. Heydenreich, P. D. Wang, and C. M. Sotomayor Torres, *Microelectron. J.* **26**, 871 (1995).
- <sup>57</sup>Z. Y. Xu, Z. D. Lu, X. P. Yang, Z. L. Yuan, B. Z. Zheng, J. Z. Xu, W. K. Ge, Y. Wang, J. Wang, and L. L. Chang, *Phys. Rev. B* **54**, 11 528 (1996).